Memory-based Model Predictive Control for Parameter Detuning in Multiphase Electric Machines

A. Gonzalez-Prieto, I. Gonzalez-Prieto, O. Dordevic, *Member, IEEE*, J.J. Aciego, J. Montenegro, M. J. Duran and M. U. Khan, *Student Member, IEEE*.

Abstract- Model predictive control (MPC) is a popular control technique to regulate multiphase electric drives (ED). Despite the well-known advantages of MPC, it is sensitive to parameter detuning and lacks the capability to eliminate steady-state errors. The appearance of an offset between the reference and measured currents can significantly jeopardize the performance of the electric drive. This work suggests the use of a memory-based model predictive control (MB-MPC) that activates a compensation term when the parameter mismatch is detected. The suggested MB-MPC is universal for any multiphase machine if spatial harmonics are neglected since the proposed method does not consider any of the secondary x-y planes. Experimental results in two different rigs with six- and nine-phase induction motors prove this universality as well as its capability to eliminate current and speed offsets.

Keywords: Model predictive control, multiphase electric drives, parameter mismatch compensation.

NOMENCLATURE

Variables

m	Number of three-phase windings
S	Switching state
v	Stator voltage
$[X]$	Vector of state variables
$[U]$	Vector of inputs of the state space
$[A],[B]$	Matrices of coefficients of state space
i	Current
U	Voltage
λ	Flux
J	Cost function
e	Error between the reference and predicted current
k	Weighting factor of the cost function
$[\Delta]$	Vector of compensation in prediction stage
N	Number of cycles recorded by the memory stage
θ	Rotor flux angle
ω_m	Mechanical speed

Subscripts

ij	Phase ij of the machine
k	Current sampling period
$k-1$	Last sampling period
$k+1$	Next sampling period
$\alpha-\beta$	Alpha and beta components
$x-y$	Secondary components
ph	Phase value

Superscripts

$*$	Reference value
$\wedge$	Predicted value
s	Stator component
r	Rotor component

I. INTRODUCTION

In the field of multiphase electric drives (EDs), modern regulation techniques such as model predictive control (MPC) are recently becoming attractive for industrial applications [1]-[3]. The first attempt to regulate a multiphase electric machine with MPC dates back to 2009 [3]. This milestone boosted the number of investigations, thus accelerating maturity of this field [3]. Apart from the inherent features of MPC (e.g., simplicity, fast dynamic response, or control flexibility), different works have shown that it is also possible to enhance the current quality [4]-[11], the fault-tolerant capability [12]-[14] or the efficiency [15]-[16]. The discrete nature of MPC has also allowed a smart selection of the control actions to avoid the so-called *average deception* [3]. In parallel, in the field of EDs some innovative operation modes have also been developed, as natural fault tolerance [17], a special braking mode [18], the series connection of voltage source converters (VSCs) [19] and the use in electric vehicles charging [20], to name a few options.

In spite of the numerous manners to improve the performance of multiphase drives, only few works have addressed the limitation of MPC to eliminate steady-state errors, especially in the event of machine parameter detuning. This lack of research is noteworthy considering that it is well-known that MPC is sensitive to parameter detuning [21]-[23]. As it will be shown in the experimental results of this investigation, the performance of MPC is satisfactory with no perceptible offsets in the current/speed tracking when the parameters of the model match those of the real motor. Nevertheless, when the machine parameters are not correctly estimated or they vary during operation, the prediction of the model becomes inaccurate, and this can degrade the control performance significantly [22]. In this regard, [22] identified the variation in the values of the rotor resistance and the mutual inductance as the main influencing factor from the perspective of the current tracking. Furthermore, conventional MPC lacks an integral stage with the capability to correct errors that are accumulated in the past; hence the predictive approach is somewhat blind and cannot suppress steady-state errors [23]. Online detuning due to saturation, thermal or deep-bar effects is common during operation [24], hence the performance of MPC can be affected and eventually lead to offsets both in the current and speed tracking (see section IV for experimental details in this regard).

Most of the research on MPC to correct steady-state errors is limited to three-phase drives [24]-[37]. In the literature, different approaches address the steady-state errors caused by parameter mismatch. For example, [26], [29] and [30] directly add an integral term. Although the prediction model is not affected, they unavoidably add some delays that may affect the control performance. A modified prediction is suggested in [25] to sum a pondered error term however this is requiring an additional tuning process. Similarly, [26] also varies the predictions including a new term related to the *q*-current, assuming that there is no error in the stator resistance. A different approach is attempted in [27] to eliminate the parameter mismatch disturbances in three-phase systems using a modified MPC with a current update mechanism. However, the proposed assumption provoked inaccuracies in the estimated parameters, particularly, in high-speed regions. In [32] a new term, tunable using a weighting factor, is added to the cost function to compensate the current tracking error. Therefore, the approach introduced in [32] requires an adequate weighting factor adjusting process. Also using a cost-function-based approach, in [33] an integral term is included in the cost function decreasing the steady-state errors under parameter mismatches. Conversely, this additional term worsen the dynamic response and increases the algorithm computational burden. On the other hand, an observer is used in [28], suggesting a somewhat complex three-step algorithm that considers the observed perturbations. The approach in [29] is to observe the machine inductances, neglecting the variation of the resistances (as in [26]). Based on this observer approach, other works, using Luenberger observer [34] or sliding-mode observer [35], predict future values of stator currents and track system disturbance caused by parameter mismatch in real time. Also, in [36]-[37], a feed-forward observer based approach is implemented to deal with lumped disturbances in the three-phase systems. Inevitably, these observer-based methods are accompanied by an inherent complexity and higher computational time.

Regarding the improvement of MPC robustness, different modern techniques have also been designed for that purpose. For instance, the important advances in the field of artificial neural networks have also been employed to improve the robustness of model predictive schemes. In this regard, [38] implemented an artificial neural network approach to estimate the weighting factors of a MPC scheme, obtaining a certain enhancement of the current tracking. However, the proposed technique is based on the usage of additional sensors. The advantages of artificial neural networks for three-phase systems were also validated in [39]. In this case the neural network was trained to replace the predictive model in the control scheme. Nevertheless, an observer dependent on machine parameters was employed to improve the robustness of the system. A recent trend in the field of electric drives from the perspective of the robustness is the development of model-free predictive schemes [40]-[42]. In fact, [40],[42] have designed different observers to improve the tracking of the reference variables when a certain parameter mismatch event appears in the system. However, regardless of the analyzed solution, the cost to be paid is a more complex system and in the case of [41] the mandatory usage of extra sensors. On the other hand, at this moment, the advantages of model-free predictive schemes have only been tested in three-phase systems.

Some attempts to enhance the current tracking in multiphase drives under parameter mismatch can be found in different works [43]-[48]. In [43] the use of an observer is suggested to modify the model parameters, improving the control robustness and minimizing the current harmonics in a six-phase drive. The method is however rather complex and requires tuning of the parameters of the additional observer. Furthermore, the method requires to be reformulated for different multiphase machines and cannot be used universally. In [44], a finite control set model predictive control (FCS-MPC), implemented in a five-phase ED, includes a discrete-time disturbance observer to enhance the robustness against the parameter mismatch. The parameter mismatches are provided by the difference between predictive errors and are included in the extended state observer. This observer is implemented with a pole placement technique, and it is required a slow time-varying parameter to reduce the complexity. Furthermore, following the extended assumption in three-phase systems (e.g., [26] or [29]), [44] neglects the variation of stator resistance as a perturbation source. The negligible importance of the stator resistance variation is also assumed in [45]; thus, pointing to the stator inductance being responsible for disturbances caused by the parameters mismatch. In [45] the use of an incremental prediction model and a discrete inductance compensation system is proposed to update the inductance value and to reduce the tracking errors. Despite the simplification, such online parameter identification method has high complexity and requires high performance controller. The approach in [46] is to include an auto-regressive term with exogenous variable (ARX) to make the drive more robust and accurate. The method is based on modifying the predictions using the past current values but, like [43], the modified version of MPC requires a tuning process to obtain the parameters of the ARX model. These parameters need to be tuned for the whole operating range, hence requiring a high number of tests to obtain parameters that perform well in different situations. In ideal case, the parameters of ARX should be variable depending on the operating point, but this would make the method even more complex. As in [43], the parameters of ARX in [46] should be estimated for each specific multiphase machine since they depend on the secondary *x*-*y* planes.

The proposal in this work is to include a memory stage that considers the past values and to activate a compensation term whenever the parameter detuning is detected. The method is termed memory-based model predictive control (MB-MPC) because it provides MPC with information from the past to detect the parameter mismatch and to correct eventual steady-state errors. The suggested MB-MPC has some attractive features, including: *i)* it does not depend on the operating point, *ii)* it does not require any MPC parameter tuning to be implemented and *iii)* it is universal, in the sense

that it can be used with no modifications in machines with any number phases, provided that the windings are distributed. Despite its simplicity, it can successfully correct the current offsets that appear under operation with machine parameter detuning. Furthermore, improved current tracking leads to an extended range of operation since the drive can reach target speeds that are not achievable with standard MPC. Finally, the universality of the proposal is verified using two different experimental rigs at different laboratories including six- and nine-phase machine.

The paper is structured as follows. Section II reviews some general considerations of multiphase EDs. Section III illustrates the structure/performance of MPC, its dependence on the machine parameters and describes the proposal of this work. Section IV provides the experimental results that validate the suitable abilities of the proposed control solution. Finally, Section V summarizes the main conclusions obtained.

II. Generalities of Multiphase Electric Drives

As previously exposed, the proposed MB-MPC is characterized by a significant universality since it can be implemented in different EDs without remarkable modifications. In this paper the universality of the algorithm is confirmed by its application on two different multiphase drives. For this reason, this section describes the foundations of multiphase EDs using a generalized approach, where the selected *n*-phase motor is formed of m three-phase windings.

In both considered EDs, each three-phase winding of the asymmetrical induction machines (IM) is fed by a two-level (2L) three-phase VSC. Therefore, for the six-phase IM where m=2, two VSCs need to be employed (see Fig. 1). In the case of the nine-phase ED (m=3), three VSCs are necessary to supply the IM, as shown in Fig. 1. The phase shift angle between the three-phase sets is $\gamma=\pi/n$ for an asymmetrical winding layout. The stator windings are connected to form m isolated neutral points.

Focusing on the VSC, the number of different switching states in each ED is 2^n. Vector S_{ij} describes the switching state behavior of each VSC leg. That is, if the upper switch of the leg is ON S_{ij}=1, and S_{ij}=0 if the opposite occurs. Regardless of the considered ED, the stator phase voltages (v_{ij}) can be estimated using the available switching states (S_{ij}), as shown in (1), where the size of the matrix is $n\times n$.

$$\begin{bmatrix} v_{a1} \\ v_{b1} \\ v_{c1} \\ \vdots \\ v_{am} \\ v_{bm} \\ v_{cm} \end{bmatrix} = \frac{V_{DC}}{3} \begin{bmatrix} 2 & -1 & -1 & 0 & 0 & 0 & & 0 & 0 & 0 \\ -1 & 2 & -1 & 0 & 0 & 0 & \cdots & 0 & 0 & 0 \\ -1 & -1 & 2 & 0 & 0 & 0 & & 0 & 0 & 0 \\ 0 & 0 & 0 & 2 & -1 & -1 & & 0 & 0 & 0 \\ 0 & 0 & 0 & -1 & 2 & -1 & \cdots & 0 & 0 & 0 \\ 0 & 0 & 0 & -1 & -1 & 2 & & 0 & 0 & 0 \\ & \vdots & & 0 & 0 & 0 & \ddots & & \vdots & \\ & & & 0 & 0 & 0 & & & & \\ & \vdots & & & \vdots & & & & \vdots & \\ 0 & 0 & 0 & 0 & 0 & 0 & 0 & 2 & -1 & -1 \\ 0 & 0 & 0 & 0 & 0 & 0 & 0 & -1 & 2 & -1 \\ 0 & 0 & 0 & 0 & 0 & 0 & 0 & -1 & -1 & 2 \end{bmatrix} \cdot \begin{bmatrix} S_{a1} \\ S_{b1} \\ S_{c1} \\ \vdots \\ S_{am} \\ S_{bm} \\ S_{cm} \end{bmatrix}, \tag{1}$$

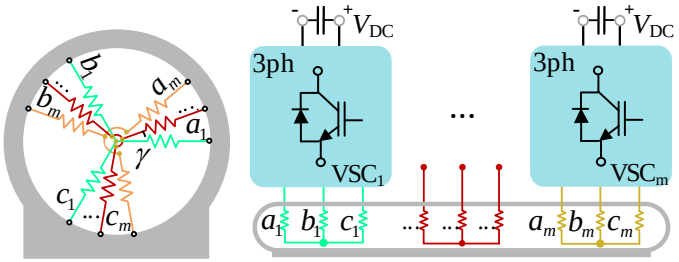

Fig. 1. n-phase asymmetrical IM fed by multiple 2L three-phase VSCs.

To avoid a complex n-dimensional mathematical study, the stator phase variables are typically expressed in diverse reference frames that facilitate the understanding and the regulation of the IM. One of the most employed reference frame transformations is the vector space decomposition (VSD) that maps the phase variables onto orthogonal subspaces expressed in a stationary reference frame [1]. For that purpose, it is a common trend in the field of EDs to make use of the amplitude-invariant Clarke transformation [23].

In this work, the VSD transformation matrices have been obtained as described in [47], considering their asymmetrical arrangements. Using Clarke's transformation, the switching states can be mapped onto all available orthogonal subspaces (see [11] for six-phase and [48] for nine-phase machine). Thus, in distributed-winding machines with negligible spatial harmonics, as in the case under study, the main subspace $(\alpha-\beta)$ is related to the flux/torque production, whereas the secondary subspaces (x_i-y_i) are solely responsible for additional stator copper losses. The number of secondary subspaces can be obtained as a function of the number of phases in the machine and the neutral point configuration. For instance, in the case of machines with isolated neutral points, the number of secondary subspaces is equal to m–1. Additionally, zero-sequence components are also present in the electric machine, but these zero-sequence currents cannot flow when employing isolated neutral points.

Focusing on control purposes, the ideal control action should achieve suitable flux/torque production with a reduced harmonic injection. However, analyzing the mapped vectors in [11] and [48], all active voltage vectors in the main plane also provoke an inherent $x-y$ injection. Searching for control actions (switching states) with an acceptable performance in the available subspaces, the role of large voltage vectors needs to be highlighted. They generate the highest voltage value in the $\alpha-\beta$ plane and a reduced contribution in the other subspaces [9], [48]. For this reason, these switching states have been selected as the active control actions in this work.

In order to regulate the flux and torque production in a decoupled form, Park transformation is commonly employed in the field of electric drives. This rotational matrix can be applied for the different subspaces:

$$[D]=\begin{bmatrix} \cos(\theta) & \sin(\theta) \\ -\sin(\theta) & \cos(\theta) \end{bmatrix},$$
$$[i_d, i_q]^T = [D]\cdot[i_\alpha, i_\beta]^T, \tag{2}$$
$$[i_{x_i}, i_{y_i}]^T = [D]^{-1}\cdot[i_{x_i}, i_{y_i}]^T,$$

where θ is the rotor flux angle, i_d is the current related to the magnetic flux production and i_q is responsible of the torque generation.

III. MPC, PARAMETER DEPENDENCE AND MB-MPC

A. Standard MPC

The standard MPC is a non-linear regulation technique characterized by the use of a machine model to carry out the current control, whereas the speed control is satisfied using a proportional-integral (PI) controller [9]. The model is formed by a set of discretized differential equations, which describe the performance of the machine, to predict the future currents. Forward Euler discretization technique [22] has been employed to model the IM behavior:

$$[\hat{X}|_{k+1}]=([I]+T_m\cdot[A])\cdot[X|_k]+T_m\cdot[B]\cdot[U|_k], \quad (3)$$

where:

$$[\hat{X}|_{k+1}]=[\hat{i}^s_\alpha|_{k+1},\hat{i}^s_\beta|_{k+1},\hat{i}^s_{x_1}|_{k+1},\hat{i}^s_{y_1}|_{k+1},...,\hat{i}^s_{x_{m-1}}|_{k+1},\hat{i}^s_{y_{m-1}}|_{k+1},\hat{\lambda}^r_\alpha|_{k+1},\hat{\lambda}^r_\beta|_{k+1}],$$

$$[X|_k]=[i^s_\alpha|_k,i^s_\beta|_k,i^s_{x_1}|_k,i^s_{y_1}|_k,...,i^s_{x_{m-1}}|_k,i^s_{y_{m-1}}|_k,\hat{\lambda}^r_\alpha|_k,\hat{\lambda}^r_\beta|_k], \quad (4)$$

$$[U|_k]=[U^s_\alpha|_k,U^s_\beta|_k,U^s_{x_1}|_k,U^s_{y_1}|_k,...,U^s_{x_{m-1}}|_k,U^s_{y_{m-1}}|_k,0,0],$$

where $[A]$ and $[B]$ are model matrices related to the machine parameters [23], $[I]$ is the identity matrix and T_m is the sampling period.

In a second prediction step, equation (3) predicts the currents that would be generated, during the next sampling period, for each available switching state. Further, the predicted currents are evaluated in a predefined cost function. In this final stage, different control objectives can be included in a simpler manner. A popular cost function for multiphase ED is the following [3]:

$$J=e_\alpha^2+e_\beta^2+k_{x_1}e_{x_1}^2+k_{y_1}e_{y_1}^2+...+k_{x_{m-1}}e_{x_{m-1}}^2+k_{y_{m-1}}e_{y_{m-1}}^2, \quad (5)$$

where:

$$e_\alpha=(i^{s*}_\alpha|_{k+2}-\hat{i}^s_\alpha|_{k+2}),\ e_\beta=(i^{s*}_\beta|_{k+2}-\hat{i}^s_\beta|_{k+2}),$$
$$e_{x_i}=(i^{s*}_{x_i}|_{k+2}-\hat{i}^s_{x_i}|_{k+2}),\ e_{y_i}=(i^{s*}_{y_i}|_{k+2}-\hat{i}^s_{y_i}|_{k+2}), \quad (6)$$

for $i\in[1,m-1]$. In (5), k_{xi} and k_{yi} are weighting factors related to the control of the secondary subspaces.

The switching state which provides the minimum cost function value is selected as the optimum control action, and it is applied to the VSC. An error in the prediction stage can lead to a sub-optimal selection of the switching state. This fact jeopardizes the performance of the regulation strategy. For that reason, it is crucial to increase the robustness of the control scheme versus possible parameter variations .

B. Impact of a parameter mismatch on the prediction process

As introduced in the previous subsection, the MPC has a strong parameter dependence because the predictive currents are obtained using $[A]$ and $[B]$. Consequently, the use of proper value of the electrical machine parameters is essential to ensure an adequate performance of MPC. Unfortunately, a parameter mismatch appears due to numerous factors, e.g., the inaccuracy of initial estimations or machine heating/saturation.

Focusing on the prediction process of MPC, characterized by (3), two different sources of errors can be identified when a possible parameter mismatch appears. The first agent is the product $[A]\cdot[X|_k]$, whereas the second source is caused by operation $[B]\cdot[U|_k]$. Both terms generate an error in the prediction process when a parameter mismatch exists. However, they show a completely different contribution to the disturbance of the control technique. Moreover, the influence of the two terms in the estimation of the currents varies according to the analyzed prediction horizon.

Regarding the first prediction step, the term $[A]\cdot[X|_k]$ varies with the measured currents in the instant k, whereas the product $[B]\cdot[U|_k]$ depends on the control action applied in the last sampling period. Therefore, the control error made due to a parameter mismatch in this prediction step can be considered as a constant value for a given sampling period. Meanwhile a different scenario appears in the second estimation horizon. On the one hand, the error produced in the first term $[A]\cdot[\hat{X}|_{k+1}]$ is still the same for all the available control actions since the vector $[\hat{X}|_{k+1}]$ is the output of the k+1 prediction step. However, this situation implies that in case of a prediction error in the first stage, it is inherited and propagated to the k+2 step. On the other hand, in the case of product $[B]\cdot[U]$, the situation is significantly different because of its input is the contribution of each available switching state in each subspace. Considering the linear nature of the $[B]$ matrix, the error increases when the voltage production of the switching state augments in the main plane. In this regard, large voltage vectors with a higher contribution in the main subspace suffer the higher disturbance in this essential plane. In exchange, this second term, i.e., $[B]\cdot[U|_k]$, does not imply any error in the prediction process for the null voltage vector. For this reason, the impact of a parameter mismatch is more profound when the operating point requires the usage of a higher percentage of active vectors.

C. Designing a MB-MPC

In order to overcome the parameter mismatch error in the standard MPC, this work proposes the use of a MB-MPC. The designed control solution is based on the reformulation of the discretized machine model including the prediction error and the usage of a memory stage to avoid false alarms. Fig. 2 shows this regulation scheme applied to an *n*-phase machine. The prediction error can be estimated in a simple manner using the difference between the predicted currents of the main subspace, provided by the prediction stage in the last sampling period, and the measured currents of the electric machine:

$$\Delta_\alpha|_k=(i^s_\alpha|_k-\hat{i}^s_\alpha|_{k-1}),$$
$$\Delta_\beta|_k=(i^s_\beta|_k-\hat{i}^s_\beta|_{k-1}). \quad (7)$$

These components are selected since, in a distributed-winding machine, only these currents produce flux and torque [22]. In case of parameter mismatch, the measured current is not equal to the predicted current obtained by the predictive model from

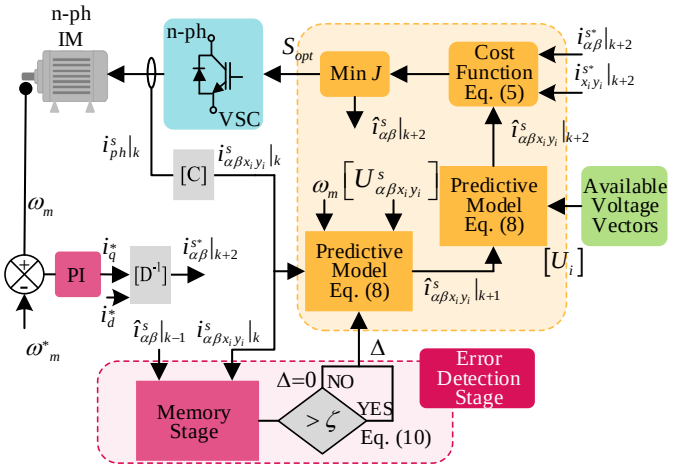

Fig. 2. Proposed MB-MPC scheme for a *n*-phase IM drive.

the previous control cycle. The difference between the expected/predicted current and the real/measured current implies a control error, causing, for instance, an inaccurate estimation of the rotor flux angle.

To avoid control errors in the main plane, the proposed MB-MPC employs a reformulated discretized machine model to be employed in the first prediction step, including the difference between the measured and the predicted current in last control period:

$$[\hat{X}|_{k+1}]=([I]+T_m\cdot[A])\cdot[X|_k]+T_m\cdot[B]\cdot[U|_k]+[\Delta|_k], \tag{8}$$

where:

$$[\Delta|_k]=\left[\Delta_\alpha|_k,\Delta_\beta|_k,0,\cdots,0\right]^T \tag{9}$$

Using this compensation technique, it is possible to surpass the prediction errors related to a parameter mismatch in a simpler manner. In addition, since the control scheme only acts over the currents mapped into the main subspace, the proposed control scheme is not dependent on the number of phases of the machine.

Nevertheless, a difference between the predicted and measured currents can appear in certain operating conditions such as a transient situation. In these circumstances, it is unnecessary to compensate the error since the source of the offset is not an electrical parameter variation. Thus, it is necessary to implement a detection algorithm to avoid these false alarm situations. Considering the previous requirement, the designed MB-MPC includes a detection stage that memorizes the difference from (7) during a specific time interval. In this way, the algorithm only considers the prediction error when the following condition is satisfied:

$$\frac{1}{N}\cdot\sum_{i=1}^{N}\sqrt{(i^s_{\alpha,i}|_k-\hat{i}^s_{\alpha,i}|_{k-1})^2+(i^s_{\beta,i}|_k-\hat{i}^s_{\beta}|_{k-1})^2}>\zeta\ , \tag{10}$$

with ζ being the modulus of the prediction error on healthy situation and N the number of control cycles recorded by the memory stage. Thanks to the use of this error detection stage the control performance is not jeopardized when the machine parameters are properly tuned or in a dynamic situation.

Focusing on the tuning of ζ, the value of this parameter is preferably determined in heathy situation and in low/speed conditions. In this scenario, the null voltage vector is selected as the optimal control action in a notable ratio. Consequently, the difference between measured and predicted currents can be considered as the inherent control error of model predictive control:

$$\zeta=\frac{1}{N}\cdot\sum_{i=1}^{N}\sqrt{(i^s_{\alpha,i}|_k-\hat{i}^s_{\alpha,i}|_{k-1})^2+(i^s_{\beta,i}|_k-\hat{i}^s_{\beta}|_{k-1})^2}\ . \tag{11}$$

In summary, the nature of the solution is simple, consider the prediction error in the last sampling period and take it into account for the next prediction stage. Finally, thanks to the detection stage, the proposed MB-MPC only acts when a prediction error is detected. Therefore, the machine performance is not degraded in healthy or dynamic situations.

IV. Experimental Results

The experimental testing of the proposed method is described in this section. For that purpose, three different scenarios have been defined on the two available EDs. Table I shows the parameters of the used EDs. The parameter mismatch event has been generated taking into account the conclusion of [22] about the importance of the different electrical parameter in the current tracking. For this reason, the values of the rotor resistance and the mutual inductance have been modified as shown in Table I. Test 1 is analyzing the ability of MB-MPC to maintain the current quality as of the conventional MPC when the model is not disturbed by the occurrence of a parameter mismatch. Nevertheless, parameter mismatches can eventually appear during the operation of an ED [22]. For that reason, Tests 2 and 3 illustrate the performance of the proposed MB-MPC when some disturbance in the parameter values occur. As it will be shown next, the simultaneous usage of both a memory stage and a compensation term has been confirmed as a suitable control solution to mitigate eventual steady-state errors.

In addition, the performance of the proposed MB-MPC has also been validated in a transient scenario. In Test 4, a speed reversal has been carried out for the nine-phase electric drive when a parameter mismatch exists. Finally, in Test 5, the suitable abilities of the designed MB-MPC to mitigate the impact of parameter mismatch are again assessed. However, in this case the control scheme of [46] is established as the basis of the comparison. This control solution is based on the usage of an exogenous variable to compensate the disturbances created by the occurrence of a parameter mismatch event.

The goodness of the proposed MB-MPC has been validated, as previously exposed, in two different test benches formed by multiple three-phase windings. In the case of the six-phase ED the control scheme is implemented in a DSP from Texas Instruments, model TMS320F28335, whereas for the nine-phase ED the real-time control system is a ds1006 of dSPACE. Therefore, the suitable performance of the proposed predictive algorithm can be confirmed regardless of the selected real-time control system or the number of phases.

A. Control scheme performance in healthy situation

This first test permits evaluating the performance of the developed MB-MPC in a healthy situation (no parameter

TABLE I
CONTROL AND N-PHASE ED PARAMETERS

Parameter	a) Healthy		b) Non healthy	
	6PH-IM	9PH-IM	6PH-IM	9PH-IM
$f_{control}$ (kHz)	10	10	10	10
ζ (A)	0.35	0.45	0.35	0.5
V_{DC} (V)	300	300	300	300
$R_s(\Omega)$	4.20	5.3	4.20	5.3
$R_r(\Omega)$	3	2	1.5	1
L_m (mH)	280	520	560	1040
L_{ls} (mH)	4.5	24	4.5	24
L_{lr} (mH)	55.1	11	55.1	11

mismatch). The memory stage allows the activation of the offset compensation term only during the steady-state error tracking. Thus, this solution shows a negligible impact on the phase currents when parameters are properly estimated, as shown in Fig. 3 and 4.

Test 1a. Six-phase electric drive

Left plots of Fig. 3 show the current regulation of the classical MPC, whereas right plots of Fig. 3 show the performance of the MB MPC for asymmetrical six-phase drive. As can be seen from Fig. 3a, the tracking of the main currents is suitable with both methods when the right values of the electrical parameters are used. Addressing the $x-y$ current regulation, the proposed strategy presents a similar behavior as the conventional MPC. Consequently, the harmonic content in phase currents is comparable for both regulation techniques.

Test 1b. Nine-phase electric drive

As in the Test 1a, left plots illustrate the performance of conventional MPC and right plots are for the proposed MB-MPC with nine-phase asymmetrical drive. The current tracking is suitable regardless of the analyzed subspace for both control schemes (Fig. 4a-c). In this case, the currents of the secondary subspaces show a lower ripple than in the six-phase case due to the higher value of the stator leakage inductance L_{ls} (see Table Ia). Remember that the model of auxiliary $x-y$ planes is composed of R_s in series with L_{ls} [2]. For that reason, the phase currents of this ED are characterized by a lower harmonic distortion when compared with analyzed six-phase drive, see Fig. 4d.

B. Control scheme performance in parameter mismatch

The aim of this second test is to illustrate the ability of the proposed method to compensate steady-state errors caused by mismatches in the prediction process due to a parameter variation. For that purpose, the values of the mutual inductance and the rotor resistance used in the prediction model are varied to include a disturbance in the predictive model. Table Ib shows the selected values of these parameters in Tests 2 and 3.

It is important to highlight that in this second test, the current tracking error does not present an impact on the speed regulation. Nevertheless, the speed tracking worsens when a higher number of active voltage vectors is selected as the optimal control actions because a high prediction error appears. As exposed in Section III, the prediction error is directly related to the amplitude of the selected voltage vector.

Test 2a. Six-phase electric drive

In this case, left plots of Fig. 5 are focused on MPC and right plots are devoted to MB-MPC. This scenario, with speed reference set to 500 rpm, lack of a memory stage and a compensation term, in the case of conventional MPC, leads to the appearance of a steady-state error in the tracking of the $\alpha-\beta$ currents, as shown in the left plot of Fig. 5b. Fortunately, this undesired situation is satisfactorily solved with the proposed MB-MPC (see Fig. 5b), where the offset is eliminated. Concerning the secondary planes components regulation, a similar performance is obtained for both control methods (Fig. 5c). Focusing on phase currents, no significant differences appear between the considered MPC methods.

Test 2b. Nine-phase electric drive

Test 2b illustrates the performance of the proposed scheme in the nine-phase ED for the parameter conditions shown in Table Ib. Left plots of Fig. 6 show the behavior of standard MPC, whereas right plots are for MB-MPC. At this operating point, both control methods can provide a suitable speed regulation (Fig. 6a), although a disturbance caused by the parameter mismatch can be seen. The situation is completely different from the perspective of current control, since a significant offset appears in the regulated currents in the main subspace, when the conventional MPC scheme is employed (see Fig. 6b-left). This undesired scenario is solved if the MB-MPC solution is implemented, as shown in Fig. 6b. In this case, the tracking of the main currents is satisfactorily carried out without jeopardizing the current quality (Fig. 6e). The minimization of the secondary currents is also suitable when the compensation term is on, see Fig. 6c and 6d.

C. Effects of no compensation under parameter mismatch

The disturbance generated by an erroneous electrical parameter estimation is directly dependent on the operating point and consequently its impact is more critical when a high output voltage is required. This third test aims to illustrate the benefits of the proposed scheme to overcome scenarios where the regulation of the speed cannot be ensured by standard MPC due to disturbance caused in the prediction process. This scenario has been generated using the electrical parameters of Table Ib.

Test 3a. Six-phase electric drive

In Test 3, the reference speed is set to 600 rpm to generate a more restrictive operating condition. Due to the erroneous current prediction, the speed regulation cannot be achieved using standard MPC, as shown in the left plot of Fig. 7a. Fortunately, in the proposed MB-MPC (right plots of Fig. 7), the control of the mechanical speed is successfully achieved because the proposed compensation term permits avoiding the appearance of any offset in the main plane currents (Fig. 7b). Therefore, the usage of the developed MB-MPC also allows the increase of the operating speed range when some disturbances appear in the values of the electrical parameters.

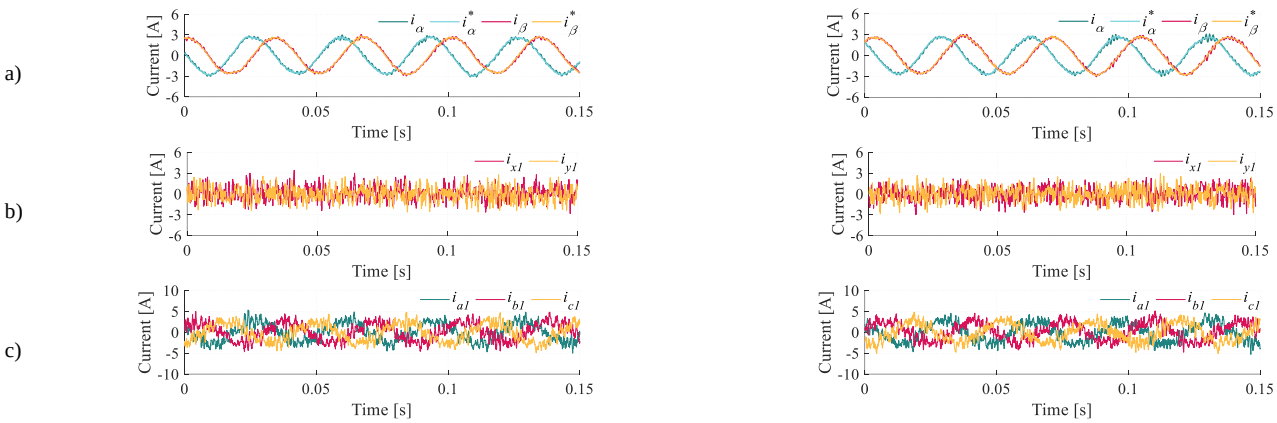

Fig. 3. Test 1a. Healthy situation for the considered six-phase ED using the standard MPC (left) and the proposed MB-MPC (right). From top to bottom: a) α - β currents, b) x_1 - y_1 currents and c) phase currents of the first winding.

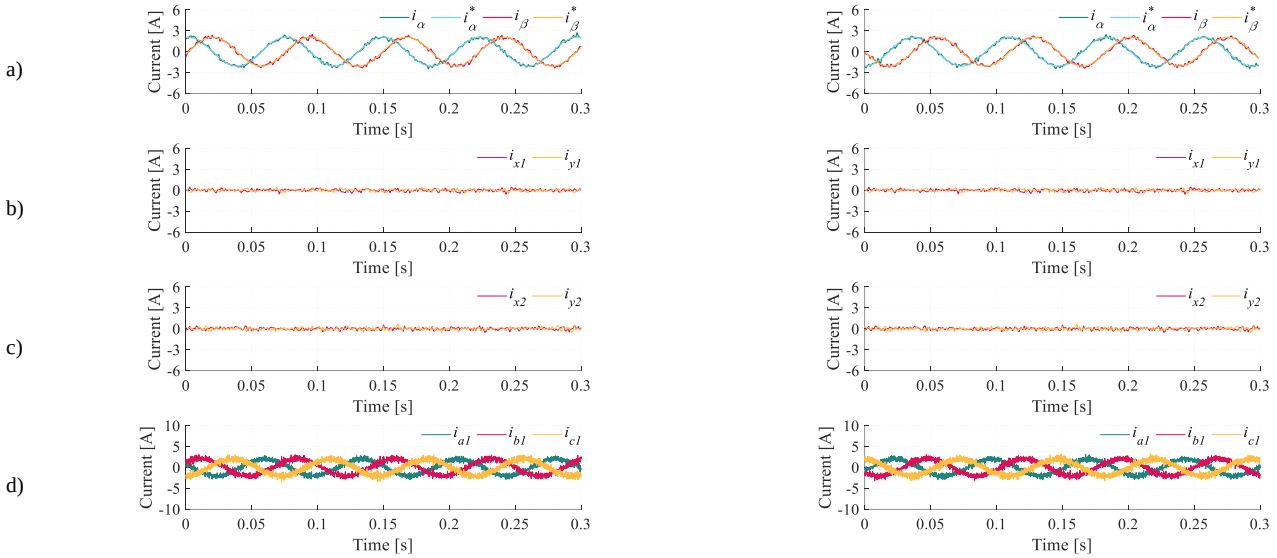

Fig. 4. Test 1b. Healthy situation for the considered nine-phase ED using the standard MPC (left) and the proposed MB-MPC (rigth). From top to bottom: a) α - β currents, b) x_1 - y_1 currents, c) x_2 - y_2 currents and d) phase currents of the first winding.

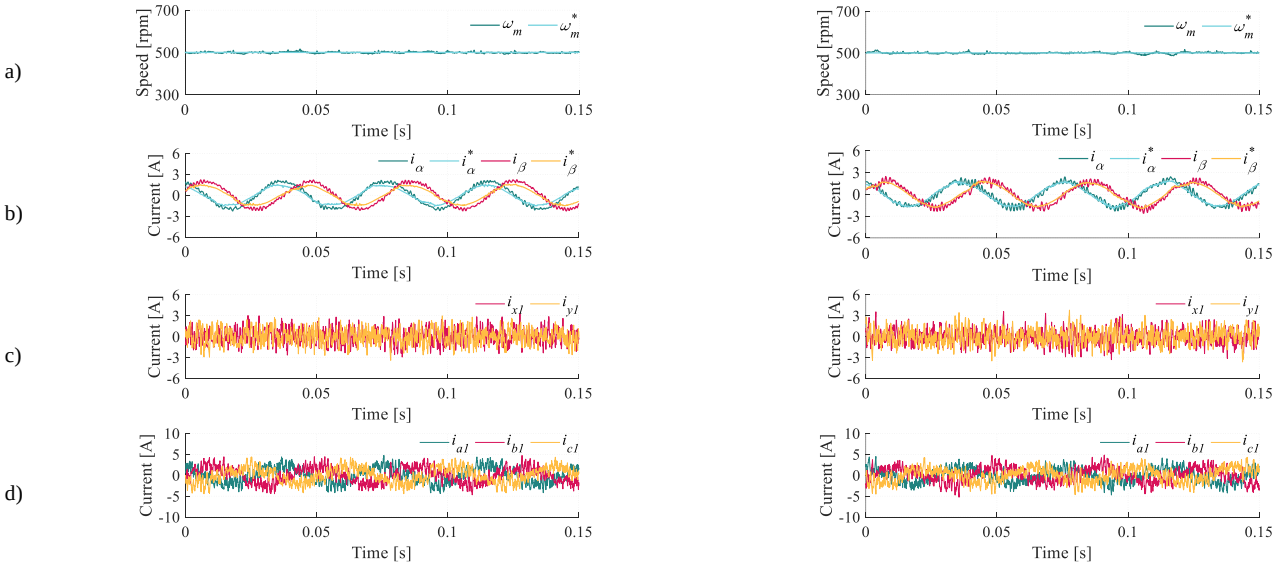

Fig. 5. Test 2a. Parameter mismatch situation for the considered six-phase ED using the standard MPC (left) and the proposed MB-MPC (rigth). From top to bottom: a) mechanical speed b) α - β currents, c) x_1 - y_1 currents and d) phase currents of the first winding.

Test 3b. Nine-phase electric drive

Following the same trend of Test 3a, the reference speed is increased up to 1200 rpm for the nine-phase ED. Due to the universality of the proposed MB-MPC, the same algorithm from Test 3a is now applied to the nine-phase machine, and once again the speed reference is properly tracked (right plot of Fig. 8a). The situation is completely different for the conventional MPC, a higher steady-state error appears in the regulation of the main plane currents and, consequently, the reference speed cannot be reached in this Test 3b. Additionally in the nine-phase ED, the mitigation of the secondary planes current components is influenced by the disorder caused in the prediction process (see left plots of Fig. 8). In order to quantify the advantages of the proposed MB-MPC over conventional FCS-MPC some control indices have been calculated and added in Table II. These results show a significant improvement in term of speed regulation. In fact, using the developed MB-MPC the speed control error has decreased 98.83 % compared to the standard version of the FCS-MPC. Focusing on the current tracking, the Mean Squared Error (MSE) has been selected as control index. In

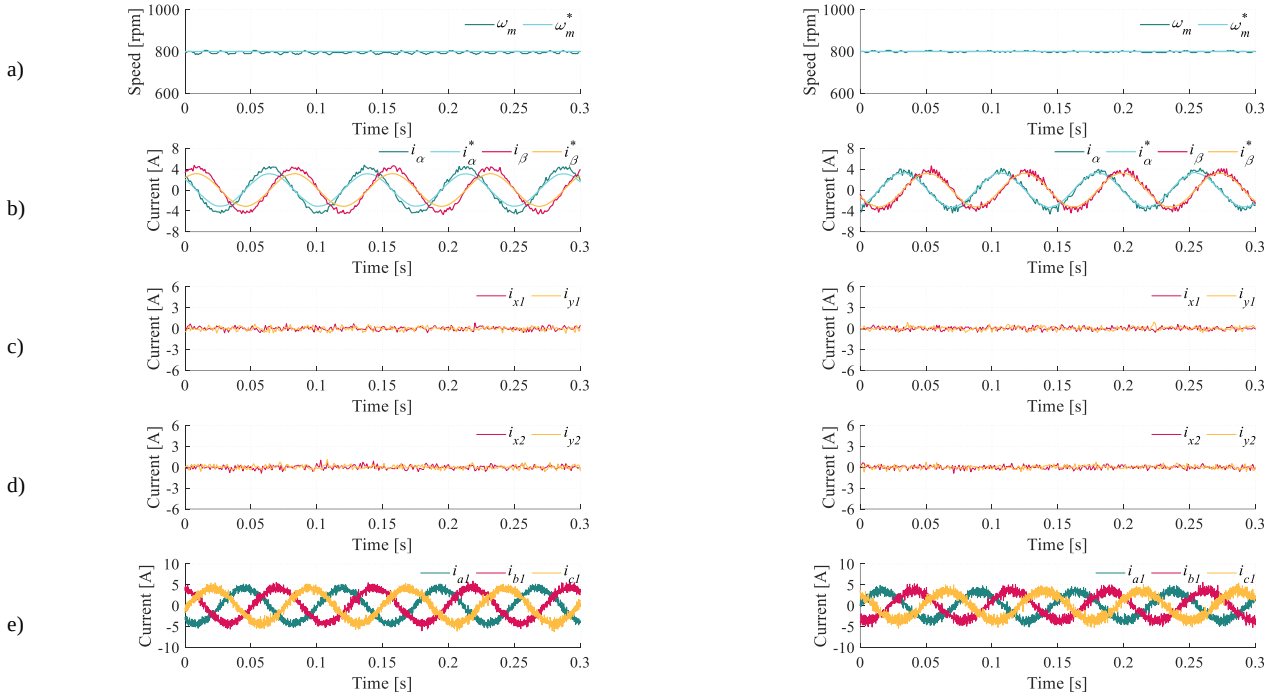

Fig. 6. Test 2b. Parameter mismatch situation for the considered nine-phase ED using the standard MPC (left) and the proposed MB-MPC (rigth). From top to bottom: a) mechanical speed b) $\alpha-\beta$ currents, c) x_1-y_1 currents, d) x_2-y_2 currents and e) phase currents of the first winding.

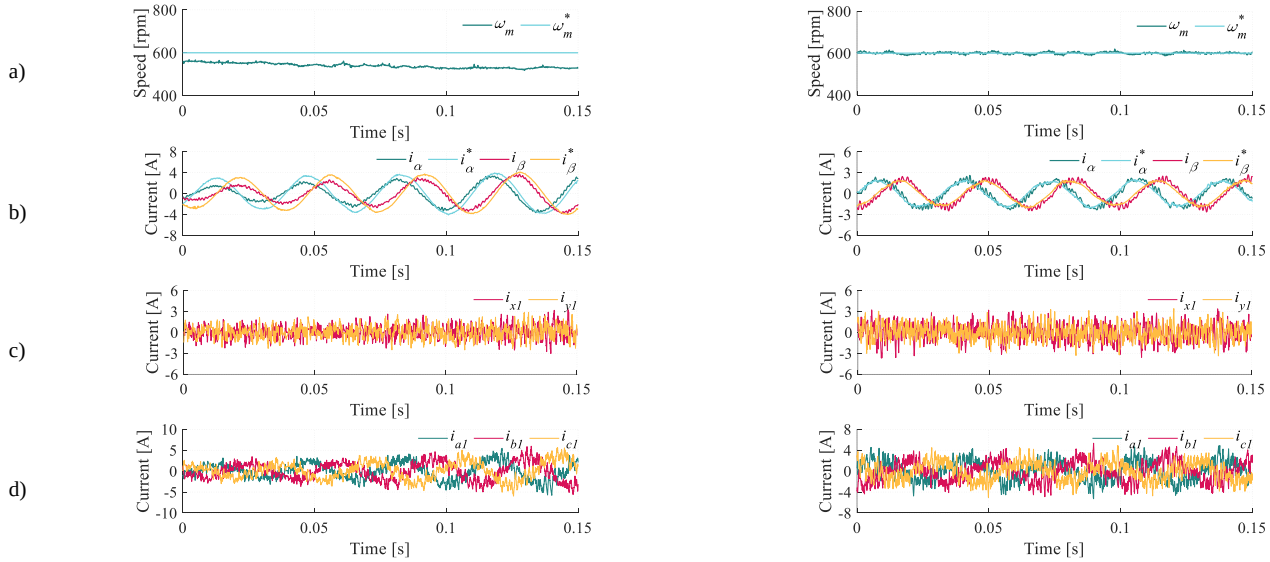

Fig. 7. Test 3a. Parameter mismatch situation for the considered six-phase ED using the standard MPC (left) and the proposed MB-MPC (rigth). From top to bottom: a) mechanical speed b) $\alpha-\beta$ currents, c) x_1-y_1 currents and d) phase currents of the first winding.

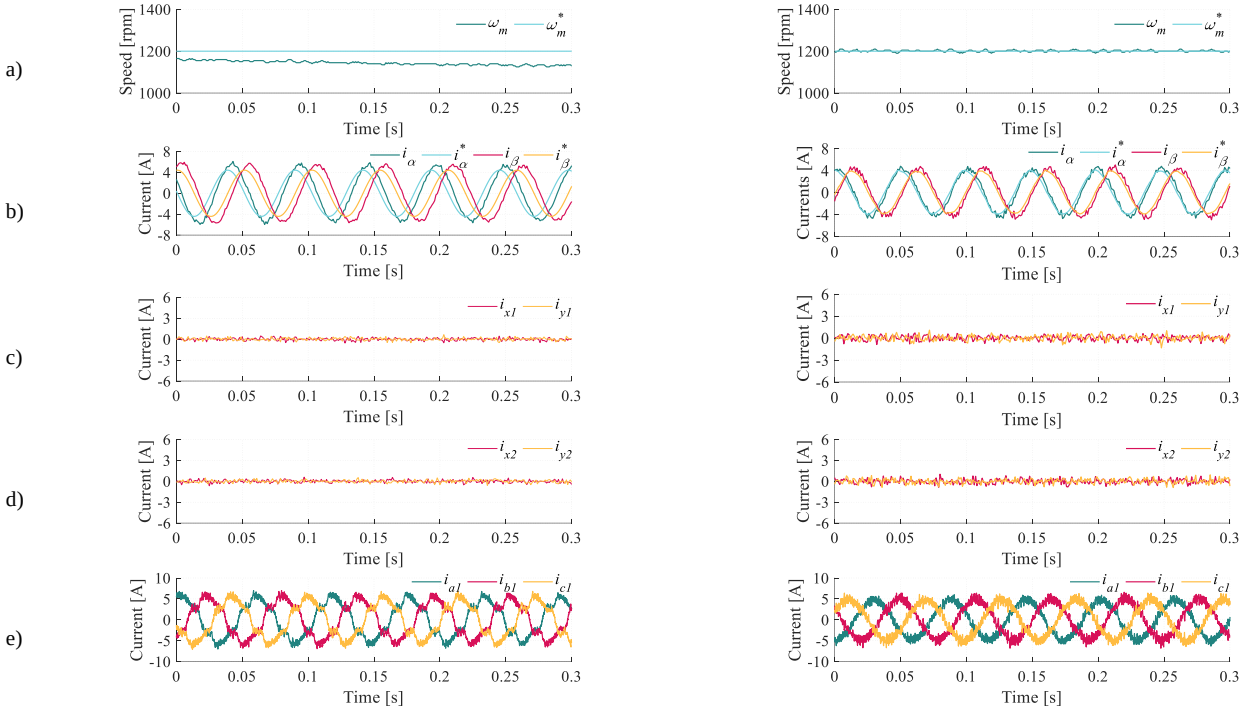

Fig. 8. Test 3b. Parameter mismatch situation for the considered nine-phase ED using the standard MPC (left) and the proposed MB-MPC (rigth). From top to bottom: a) mechanical speed b) $\alpha-\beta$ currents, c) x_1-y_1 currents, d) x_2-y_2 currents and e) phase currents of the first winding.

TABLE II.
SPEED AND CURRENT CONTROL ERROR

Variable error	Standard FCS-MPC	MB-MPC
Lineal control error of ω_m	67.3926 rpm	0.7842 rpm
Mean Squared error of $\alpha-\beta$	6.4458 A	0.7952 A

this regard, the designed MB-MPC produces a reduction of 87.7% of the MSE in comparison to conventional MPC.

D. Dynamic scenario and parameter mismatch

Test 4 shows the response of the MB-MPC in the nine-phase electric drive when a speed step from -800 rpm to 800 rpm is set. To verify the error compensation of the proposed regulation technique, a variation in the parameters has been included. Specifically, the mutual inductance and the rotor resistance are modified according to Table I. As shown in Fig. 9, even in the presence of a parameter mismatch, the proposed MB-MPC successfully tracks the reference speed since there is no observable control error in the main currents. In terms of secondary currents, there is no effect in their control when a dynamic situation occurs (Figs. 9c and 9d). As it can be seen in Fig. 9, the compensation of the parameter mismatch is carried out without affecting the dynamic performance.

E. Comparison with an autoregressive method

The goal of Test 5 is to illustrate the advantages of the proposed MB-MPC in comparison with available control solutions that also focus on the robustness of model-based predictive strategies. Based on the mentioned purpose, the regulation approach developed in [46] has been selected as a basis of the comparison. Fig. 10 shows the results of both control techniques when they are implemented in the six-phase ED in a parameter mismatch scenario. As shown in Fig. 10, the designed MB-MPC provides a better tracking of the main currents, achieving in addition a lower ripple of the waveform of these components.

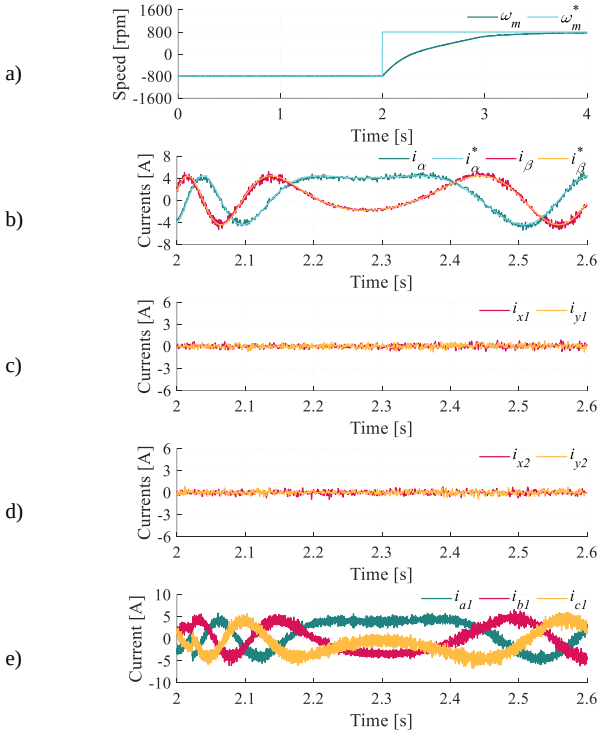

Fig. 9. Speed reversal test for the proposed control scheme MB-MPC. From top to bottom: a) mechanical speed, b) $\alpha-\beta$ currents, c) x_1-y_1 currents, d) x_2-y_2 currents and e) phase current of the first winding.

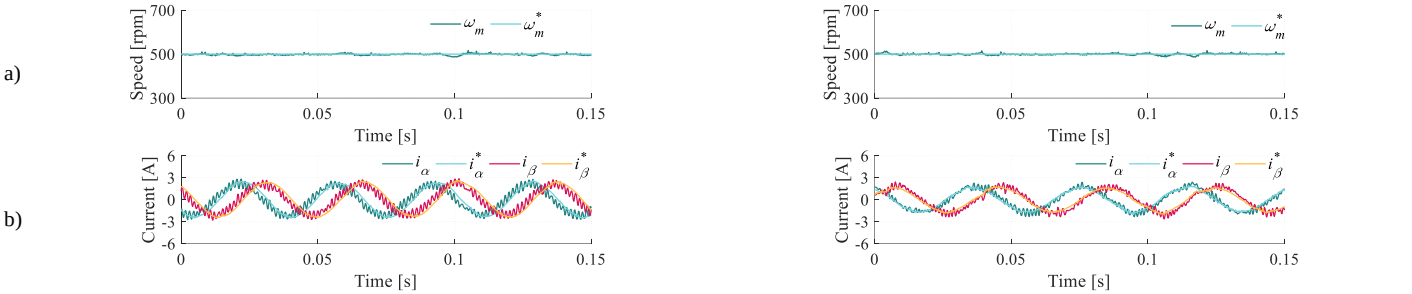

Fig.10. Parameter mismatch situation for the considered six-phase electric drives using MPC including ARX disturbance estimator [46] (left column) and MB-MPC (rigth column). From top to bottom: a) mechanical speed and b) $\alpha-\beta$ currents.

V. CONCLUSIONS

Standard MPC cannot eliminate steady-state errors when machine parameter detuning exists. In fact, an offset between the reference and measured currents appears in the event of a parameter mismatch. Poor current tracking leads in turn to a reduced operating speed range, since the control is unable to follow the reference speed when high voltages are required.

To overcome this limitation, this work proves that the inclusion of a compensation term in the proposed MB-MPC structure can successfully eliminate steady-state current errors. Moreover, the proposal provides a satisfactory speed tracking in operating points unreachable by standard MPC. Thus, the suggested MB-MPC simultaneously achieves a proper current and speed tracking with no visible offsets even at high-speed operating points. The memory stage that is included in the proposal allows activating the compensation term only when a parameter mismatch or a disturbance provoke a difference between the reference and measured currents, maintaining standard MPC otherwise. Furthermore, the compensation term that corrects the steady-state errors only affects the main subspace, hence the method is universal for any distributed-winding multiphase machine. Experimental results on six- and nine-phase multiphase EDs confirm this statement and shows the capability of MB-MPC to achieve a correct current/speed tracking both in normal and detuned operation.

REFERENCES

[1] M. J. Duran, E. Levi, and F. Barrero, "Multiphase electric drives: Introduction," *Wiley Encyclopedia of Electr. and Electron. Eng.*, J. G. Webster, Ed., 2017

[2] E. Levi, R. Bojoi, F. Profumo, H. A. Toliyat, and S. Williamson, "Multiphase induction motor drives: A technology status review," *IET Electr. Power Appl.*, vol. 1, no. 4, pp. 489–516, 2007.

[3] M. J. Duran, I. Gonzalez-Prieto, A. Gonzalez-Prieto and J. J. Aciego, "The evolution of model predictive control in multiphase electric drives: A Growing Field of Research," *IEEE Ind. Electron. Mag.*, vol. 16, no. 4, pp. 29-39, 2022.

[4] A. Shawier, A. Habib, M. Mamdouh, A. S Abdel-Khalik and K. H. Ahmed, "Assessment of predictive current control of six-phase IM with different winding configurations," *IEEE Access*, vol. 9, pp. 81125-81138, 2021.

[5] C. Xue, W. Song, X. Wu, and X. Feng, "A constant switching frequency finite-control-set predictive current control scheme of a five-phase inverter with duty-ratio optimization," *IEEE Trans. Power Electron*., vol. 33, no. 4, pp. 3583–3594, 2018.

[6] Y. Luo and C. Liu, "Multi-vectors-based model predictive torque control for a six-phase PMSM motor with fixed switching frequency," *IEEE Trans. Energy Convers.*, vol. 34, no. 3, pp. 1369–1379, 2019.

[7] M. Ayala, et al., "A novel modulated model predictive control applied to six-phase induction motor drives," *IEEE Trans. Ind. Electron.*, vol. 68, no. 5, pp. 3672–3682, 2021.

[8] A. Gonzalez-Prieto, I. Gonzalez-Prieto, and M. J. Duran, "Smart voltage vectors for model predictive control of six-phase electric drives," *IEEE Trans. Ind. Electron.*, vol. 68, no. 10, pp. 9024–9035, 2021.

[9] J. J. Aciego, I. Gonzalez Prieto, M. J. Duran, M. Bermudez, and P. Salas-Biedma, "Model predictive control based on dynamic voltage vectors for six-phase induction machines, " *IEEE J. Emerg. Sel. Topics Power Electron.*, vol.9, no. 3, pp. 2710–2722, 2021.

[10] P. Goncalves, S. M. A. Cruz, and A. M. S. Mendes, "Multistage predictive current control based on virtual vectors for the reduction of current harmonics in six-phase PMSMs," *IEEE Trans. Energy Convers.*, vol. 36, no. 2, pp. 1368–1377, 2021.

[11] A. Gonzalez-Prieto et al., "Hybrid multivector FCSMPC for six-phase electric drives," *IEEE Trans. Power Electron.*, vol. 37, no. 8, pp. 8988-8999, 2022.

[12] B. Chikondra, U. R. Muduli and R. K. Behera, "An improved open-phase fault-tolerant DTC technique for five-phase induction motor drive based on virtual vectors assessment," *IEEE Trans. Ind. Electron.*, vol. 68, no. 6, pp. 4598-4609, 2021.

[13] Y. Luo and C. Liu, "Pre- and Post-Fault Tolerant Operation of a Six-Phase PMSM Motor Using FCS-MPC Without Controller Reconfiguration," *IEEE Trans. Veh. Technol.*, vol. 68, no. 1, pp. 254-263, 2019.

[14] M. Salehifar, R. S. Arashloo, J. M. Moreno-Equilaz, V. Sala and L. Romeral, "Fault detection and fault tolerant operation of a five-phase pm motor drive using adaptive model identification approach," *IEEE J. Emerg. Sel. Topics Power Electron.*, vol. 2, no. 2, pp. 212-223, 2014.

[15] B. Yu, W. Song, K. Yang, Y. Guo and M. S. R. Saeed, "A Computationally Efficient Finite Control Set Model Predictive Control for Multiphase PMSM Drives," *IEEE Trans. Ind. Electron.*, vol. 69, no. 12, pp. 12066-12076, 2022.

[16] M. S. R. Saeed, W. Song, B. Yu and X. Wu, "Low-Complexity deadbeat model predictive current control with duty ratio for five-phase PMSM drives," *IEEE Trans. Ind. Electron*, vol. 35, no. 11, pp. 12085-12099, 2020.

[17] I. G. Prieto, M. J. Duran, P. Garcia-Entrambasaguas and M. Bermudez, "Field-oriented control of multiphase drives with passive fault tolerance," *IEEE Trans. Ind. Electron*, vol. 67, no. 9, pp. 7228-7238, 2020.

[18] M. J. Duran et al., "A simple braking method for six-phase induction motor drives with unidirectional power flow in the base-speed region," *IEEE Trans. Ind. Electron*, vol. 64, no. 8, pp. 6032-6041, 2017.

[19] H. S. Che et al., "Operation of a six-phase induction machine using series-connected machine-side converters," *IEEE Trans. Ind. Electron*, vol. 61, no. 1, pp. 164-176, 2014.

[20] I. Subotic, N. Bodo and E. Levi, "An EV drive-train with integrated fast charging capability," *IEEE Trans. Power Electron.*, vol. 31, no. 2, pp. 1461-1471, 2016.

[21] H. A. Young, M. A. Perez and J. Rodriguez, "Analysis of FCS-MPCC with model parameter mismatch in a three-phase inverter," *IEEE Trans. Ind. Electron.*, vol.63, no.5, pp. 3100-3107, 2016.

[22] C. Martin et al., "Sensitivity of predictive controllers to parameter variation in five-phase induction motor drives," *Control Eng. Pract.*, vol. 68, pp. 23-31, 2017.

[23] A. Gonzalez-Prieto, I. Gonzalez-Prieto, M. J. Duran, and J. J. Aciego, "Dynamic response in multiphase electric drives: control performance and influencing factors," *Machines*, vol. 10, no. 10, p. 866, 2022.

[24] M. Abdelrahem, C. M. Hackl, R. Kennel and J. Rodríguez, "Efficient direct-model predictive control with discrete-time integral action for PMSGs," *IEEE Trans. Energy Convers.*, vol. 34, no. 2, pp. 1063-1072, 2019.

[25] M. Siami, D. A. Khaburi, A. Abbaszadeh and J. Rodríguez, "Robustness Improvement of predictive current control using prediction error correction for permanent-magnet synchronous machines," *IEEE Trans. Ind. Electron.*, vol. 63, no. 6, pp. 3458-3466, 2016.

[26] M. Siami, D. A. Khaburi and J. Rodríguez, "Torque ripple reduction of predictive torque control for PMSM drives with parameter mismatch," *IEEE Trans. Power Electron.*, vol. 32, no. 9, pp. 7160-7168, 2017.

[27] X. Yuan, S. Zhang and C. Zhang, "Improved model predictive current control for SPMSM drives with parameter mismatch," *IEEE Trans. Ind. Electron.*, vol. 67, no. 2, pp. 852-862, 2020.

[28] J. Wang, F. Wang, Z. Zhang, S. Li and J. Rodríguez, "Design and implementation of disturbance compensation-based enhanced robust finite control set predictive torque control for induction motor systems," *IEEE Trans. Industr. Inform.* , vol. 13, no. 5, pp. 2645-2656, 2017.

[29] X. Zhang, L. Zhang and Y. Zhang, "Model predictive current control for PMSM drives with parameter robustness improvement," *IEEE Trans. Power Electron.*, vol. 34, no. 2, pp. 1645-1657, 2019.

[30] H. Le-Huy, K. Slimani, and P. Viarouge, "Analysis and implementation of a real-time predictive current controller for permanent-magnet synchronous servo drives," *IEEE Trans. Ind. Electron*., vol. 41, no. 1, pp. 110–117, 1994.

[31] C. Xu, Z. Han, and S. Lu, "Deadbeat predictive current control for permanent magnet synchronous machines with closed-form error compensation," *IEEE Trans. Power Electron*., vol. 35, no. 5, pp. 5018–5030, 2020.

[32] M. Norambuena, P. Lezana and J. Rodriguez, "A method to eliminate steady-state error of model predictive control in power electronics," *IEEE J. Emerg. Sel. Topics Power Electron.*, vol. 7, no. 4, pp. 2525-2530, 2019.

[33] X. Liu et al., "Robust predictive current control of permanent-magnet synchronous motors with newly designed cost function," *IEEE Trans. Power Electron*., vol. 35, no. 10, pp. 10778–10788, 2020.

[34] B. Wang, X. Chen, Y. Yu, G. Wang and D. Xu, "Robust predictive current control with online disturbance estimation for induction machine drives," *IEEE Trans. Power Electron*., vol. 32, no. 6, pp. 4663-4674, 2017.

[35] F. Wang et al., "Finite control set model predictive torque control of induction machine with a robust adaptive observer," *IEEE Trans. Ind. Electron*., vol. 64, no. 4, pp. 2631–2641, 2017.

[36] L. Yan, M. Dou, Z. Hua, H. Zhang, and J. Yang, "Robustness improvement of FCS-MPTC for induction machine drives using disturbance feedforward compensation technique," *IEEE Trans. Power Electron*., vol. 34, no. 3, pp. 2874–2886, 2019.

[37] J. Wang, F. Wang, G. Wang, S. Li and L. Yu, "Generalized Proportional integral observer based robust finite control set predictive current control for induction motor systems with time-varying disturbances," *IEEE Trans. Industr. Inform.*, vol. 14, no. 9, pp. 4159-4168, 2018.

[38] T. Dragičević and M. Novak, "Weighting Factor Design in Model Predictive Control of Power Electronic Converters: An Artificial Neural Network Approach," *IEEE Trans. Ind. Electron.*, vol. 66, no. 11, pp. 8870-8880, Nov. 2019.

[39] D. Wang et al., "Model Predictive Control Using Artificial Neural Network for Power Converters," *IEEE Trans. Ind. Electron.*, vol. 69, no. 4, pp. 3689-3699, April 2022

[40] J. Wang, F. Wang, Z. Zhang, S. Li and J. Rodríguez, "Design and Implementation of Disturbance Compensation-Based Enhanced Robust Finite Control Set Predictive Torque Control for Induction Motor Systems," *IEEE Trans. Ind. Inform.*, vol. 13, no. 5, pp. 2645-2656, Oct. 2017.

[41] Kyeong-Hwa Kim and Myung-Joong Youn, "A simple and robust digital current control technique of a PM synchronous motor using time delay control approach," *IEEE Trans. Power Electron*., vol. 16, no. 1, pp. 72-82, Jan. 2001.

[42] Y. A. -R. I. Mohamed and E. F. El-Saadany, "Robust High Bandwidth Discrete-Time Predictive Current Control with Predictive Internal Model—A Unified Approach for Voltage-Source PWM Converters," *IEEE Trans. Power Electron*., vol. 23, no. 1, pp. 126-136, Jan. 2008.

[43] P. F. C. Gonçalves, S. M. A. Cruz and A. M. S. Mendes, "Disturbance observer based predictive current control of six-phase permanent magnet harmonics," *IEEE Trans. Ind. Electron.*, vol. 69, no. 1, pp. 130-140, 2022.

[44] C. Xiong, H. Xu, T. Guan, and P. Zhou, "A constant switching frequency multiple-vector-based model predictive current control of five-phase PMSM with nonsinusoidal back EMF," *IEEE Trans. Ind. Electron.*, vol. 67, no. 3, pp. 1695–1707, 2020.

[45] S. Liu and C. Liu, "Virtual-vector based robust predictive current control for dual three-phase PMSM," *IEEE Trans. Ind. Electron.*, vol. 68, no. 3, pp. 2048–2058, 2021.

[46] M. Bermudez, M. R. Arahal, M. J. Duran, and I. Gonzalez-Prieto, "Model predictive control of six-phase electric drives including ARX disturbance estimator," *IEEE Trans. Ind. Electron.*, vol. 68, no. 1, pp. 81–91, 2021.

[47] I. Zoric, M. Jones and E. Levi, "Vector space decomposition algorithm for asymmetrical multiphase machines," *2017 Int. Symp. on Power Electron. (Ee)*, Novi Sad, Serbia, 2017, pp. 1-6.

[48] P. Garcia-Entrambasaguas, I. Zoric, I. González-Prieto, M. J. Duran and E. Levi, "Direct torque and predictive control strategies in nine-phase electric drives using virtual voltage vectors," *IEEE Trans. on Power Electron*, vol. 34, no. 12, pp. 12106-12119, 2019.